 Inorg. Chem. **1987**, *26*, 3878–3886

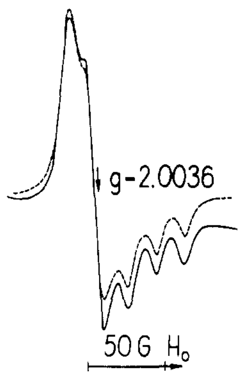

Figure 8. EPR spectrum of PC (g_0 = 2.001) observed after finishing of the reaction of $Pd_3(OAc)_5O_2$ with ethylene in C_6H_6 (the samples contain the $Pd(OAc)(NO_2)$ impurity) in the frozen-benzene solution (T = 77 K). The dotted line corresponds to a simulated spectrum.

values of g and A)[44] and suggest that we are dealing with a radical bound to a metal ion.

Interestingly, the formation of the triplet (g_0 = 2.001) was not observed if ethanol (concentration $\lesssim$ 0.3 M) had been added to the reaction mixture prior to the beginning of the reaction. Meanwhile, the addition of EtOH after the formation of the PCs with g_0 = 2.001 did not lead to their decay. It seems that Pd–O$^\bullet$ more rapidly reacts with ethanol than with $Pd(OAc)(NO_2)$ so that the nitrogen-containing free radical is not formed in the presence of ethanol. In contrast to PdO$^\bullet$, the PC with g_0 = 2.001 is quite stable. It does not react with ethanol, and its EPR signal remains unchanged, after the mixture is boiled in benzene for 5 min.

Thus, all the data discussed in this section are in agreement with the proposed mechanism of ethylene oxidation by palladium superoxo complexes via eq 3.

(44) Atkins, P. W.; Symons, M. C. R. *The Structure of Inorganic Radicals*; Elsevier: Amsterdam, London, New York, 1967.

Conclusions

1. The interaction of palladium complexes such as $Pd(OAc)_2$, $Pd(OPr)_2$, $Pd(OOCCF_3)_2$, $Pd(acac)_2$, and $Pd(PPh_3)_4$ with H_2O_2 or KO_2 in various solvents produces superoxo complexes of two types—type I and type II. The difference in the g values and reactivity of complexes belonging to different types can be explained by assuming different types of O_2^- coordination to the metal (η^1 coordination for superoxo complexes of type I and η^2 coordination for those of type II). Coordination of η^1 appears to be characteristic of trimeric Pd complexes, while η^2 is characteristic of monomeric Pd complexes.

2. Superoxo complexes of type I oxidize alkenes and carbon monoxide. Those of type II are inert with regard to these compounds. Superoxo complexes of type I with the proposed structure $Pd_3(OAc)_5O_2^\bullet$ (η^1) rapidly oxidize ethylene to ethylene oxide, 1 $\pm$ 0.1 mol of ethylene oxide being formed per 1 $\pm$ 0.3 mol of the superoxo complex consumed, and propylene to propylene oxide and acetone in a 1:2 ratio.

Registry No. $Pd(acac)_2$, 14024-61-4; $Pd(PPh_3)_4$, 14221-01-3; $Pd_3(OAc)_6$, 53189-26-7; $Pd_3(OPr)_6$, 81352-62-7; 18-crown-6, 17455-13-9; ethylene, 74-85-1; propylene, 115-07-1; isobutylene, 115-11-7; tetramethylethylene, 563-79-1; carbon monoxide, 630-08-0; ethylene oxide, 75-21-8; propylene oxide, 75-56-9; acetone, 67-64-1.

Contribution from the Departments of Chemistry, Tulane University, New Orleans, Louisiana 70118, and Washington State University, Pullman, Washington 99164

Synthesis, Reactivity, Kinetics, and Photochemical Studies on Tetrakis(μ-pyrophosphito)diplatinate(II) and Dihalotetrakis(μ-pyrophosphito)diplatinate(III) Complexes. Comparison of the Substitution Mechanisms of the Diplatinum(III) Complexes with Those of Monomeric Platinum(II) and Platinum(IV) Compounds[1]

Samuel A. Bryan,[2a] Mark K. Dickson,[2b] and D. Max Roundhill*[2a]

Received April 16, 1987

The diplatinum(II) complex $K_4[Pt_2(\mu\text{-}P_2O_5H_2)_4]\cdot 2H_2O$ with the bridging pyrophosphito-*P,P'* dianion has been synthesized by fusion of K_2PtCl_4 with phosphorous acid. Addition of halogens X_2 gives the diplatinum(III) complexes $K_4[Pt_2(\mu\text{-}P_2O_5H_2)_4X_2]$ (X = Cl, Br, I). The mixed-halide complexes $Pt_2(\mu\text{-}P_2O_5H_2)_4XY^{4-}$ can be prepared in solution by treating $Pt_2(\mu\text{-}P_2O_5H_2)_4^{4-}$ with halogen X_2 in the presence of halide ion Y^- at low pH (X = I, Y = Cl, Br; X = Br, Y = Cl). Characterization methods include ^{31}P and ^{195}Pt NMR, UV–vis, and IR spectroscopy. The complex $Pt_2(\mu\text{-}P_2O_5H_2)_4^{4-}$ is a dibasic acid, and the complexes $Pt_2(\mu\text{-}P_2O_5H_2)_4X_2^{4-}$ are tribasic acids. Rate data have been collected for the replacement of Cl^- in $Pt_2(\mu\text{-}P_2O_5H_2)_4Cl_2^{4-}$ by I^- and Br^- and for the replacement of Br^- in $Pt_2(\mu\text{-}P_2O_5H_2)_4Br_2^{4-}$ by I^-. In each case the reaction is catalyzed by added $Pt_2(\mu\text{-}P_2O_5H_2)_4^{4-}$. For the replacement of Cl^- in $Pt_2(\mu\text{-}P_2O_5H_2)_4Cl_2^{4-}$ by I^-, k_{obsd} is linearly dependent on $[Pt_2(\mu\text{-}P_2O_5H_2)_4^{4-}]$, but the plot against $[I^-]$, which is linear at low $[I^-]$, becomes independent of $[I^-]$ at high $[I^-]$. The reaction is inhibited by added Cl^-. Removal of the catalyst $Pt_2(\mu\text{-}P_2O_5H_2)_4^{4-}$ with added iodine allows measurement of the second-order associative interchange or reductive-elimination–oxidative-addition (REOA) rate constant, 1.4 (2) $\times$ 10^{-3} M^{-1} s^{-1}, and the first-order dissociative rate constant, 8.9 (10) $\times$ 10^{-6} s^{-1}. The data for the catalyzed pathway can be fitted to a mechanism involving a preequilibrium between I^- and $Pt_2(\mu\text{-}P_2O_5H_2)_4^{4-}$, followed by reaction between $Pt_2(\mu\text{-}P_2O_5H_2)_4I^{5-}$ and $Pt_2(\mu\text{-}P_2O_5H_2)_4Cl_2^{4-}$. The association between $Pt_2(\mu\text{-}P_2O_5H_2)_4^{4-}$ and I^- in aqueous solution has been independently observed by UV–vis and ^{195}Pt NMR spectroscopy and also by calorimetry. The kinetics of the replacement of Cl^- in $Pt_2(\mu\text{-}P_2O_5H_2)_4Cl_2^{4-}$ by Br^- can be explained by assuming a preequilibrium between $Pt_2(\mu\text{-}P_2O_5H_2)_4^{4-}$ and $Pt_2(\mu\text{-}P_2O_5H_4)_4Cl_2^{4-}$, followed by reaction of $Pt_2(\mu\text{-}P_2O_5H_2)_4ClPt_2(\mu\text{-}P_2O_5H_2)_4Cl^{8-}$ with Br^-. Plots of k_{obsd} against $[Pt_2(\mu\text{-}P_2O_5H_2)_4^{4-}]$ show a linear dependence at low concentrations, but decreased dependence at larger values. For the replacement of Br^- in $Pt_2(\mu\text{-}P_2O_5H_2)_4Br_2^{4-}$ by I^-, we observe linear plots of k_{obsd} against both $[Pt_2(\mu\text{-}P_2O_5H_2)_4^{4-}]$ and $[I^-]$. These substitution reactions are all accelerated by light. For the photoconversion between $Pt_2(\mu\text{-}P_2O_5H_2)_4Cl_2^{4-}$ and $Pt_2(\mu\text{-}P_2O_5H_2)_4I_2^{4-}$ with added halide ions (I^- or Cl^-, respectively), the quantum yields are low (ϕ = 10^{-3}–10^{-6}). The reaction pathway is proposed to involve the formation of a labile excited-state intermediate $d\sigma^1 d\sigma^{*1}$ that has a homolytically cleaved Pt(III)–Pt(III) bond. The respective quantum yields for the reductive elimination of X_2 from $Pt_2(\mu\text{-}P_2O_5H_2)_4X_2^{4-}$ are 7.3 (1) $\times$ 10^{-4}, 1.8 (1) $\times$ 10^{-4}, and 1.1 (1) $\times$ 10^{-5} for X = Cl, Br, and I.

Interest in the synthesis, structure, spectroscopy, and reaction chemistry of bimetallic transition-metal complexes continues to grow. The major focus of the majority of these studies is structural or spectroscopic, and there is little published work that quanti-

0020-1669/87/1326-3878$01.50/0

tatively estimates the effect of more than a single metal on chemical reactivity. Although individual systems have been investigated, no series of bimetallic complexes has yet been studied where the kinetics and mechanisms of the thermal and photochemical reactions can be directly compared with those of the monomeric analogues. This void is partly due to the lack of mechanistic and kinetic studies on bimetallic complexes, but a second reason is the unavailability of systems where the monomeric analogues have also been studied in broad detail. This paper reports a kinetic study of the substitution chemistry of μ-pyrophosphito diplatinum(III) complexes, and from the results we make a comparison with the thermal and photochemical substitution chemistry of monomeric platinum(II) and -(IV) complexes.

When potassium tetrachloroplatinate(II) is fused with phosphorous acid the μ-pyrophosphito-*P,P'* complex $K_4[Pt_2(\mu\text{-}P_2O_5H_2)_4]\cdot 2H_2O$ is formed.[3] This complex has an eclipsed "lantern" type structure with nonbonded platinum centers at a distance of 2.925 (1) Å.[4] The complex adds halogens X_2 (X = Cl, Br, I) to give the axially substituted diplatinum(III) complexes $Pt_2(\mu\text{-}P_2O_5H_2)_4X_2^{4-}$.[5] The presence of two platinum centers in these μ-pyrophosphito complexes causes significant spectroscopic differences from monomeric platinum complexes. A simplified molecular orbital treatment of binuclear d^8 complexes proposed by Gray[6] considers that the close separation between metal centers causes the filled d_{z^2} orbitals on each metal to interact and form filled bonding and antibonding orbitals. This intermetallic interaction causes the filled antibonding $^1A_{1g}(d\sigma^*)$ orbital to become closer in energy separation to the empty $^1A_{2u}(p_z)$ orbital, and consequently the absorption spectrum of $Pt_2(\mu\text{-}P_2O_5H_2)_4^{4-}$ shows bands at 367 nm ($\epsilon = 3.45 \times 10^4$ mol^{-1} dm^3 cm^{-1}; $^1A_{2u} \leftarrow {}^1A_{1g}$) and 452 nm ($\epsilon = 1.1 \times 10^2$ mol^{-1} dm^3 cm^{-1}; $^3A_{2u} \leftarrow {}^1A_{1g}$).[7] Halogen addition to form the Pt^{III}_2 complexes involves loss of the $d\sigma^*$ electrons, and intense absorption bands for $d\sigma^* \leftarrow d\sigma$ or LMCT transitions are found in all $Pt_2(\mu\text{-}P_2O_5H_2)_4X_2^{4-}$ complexes.

A vibrational Raman study of the complexes $Pt_2(\mu\text{-}P_2O_5H_2)_4^{4-}$ and $Pt_2(\mu\text{-}P_2O_5H_2)_4XY^{4-}$ (X = Y = Cl, Br, I; X = CH_3, Y = I) has concluded that there is little intermetallic bonding in the Pt^{II}_2 compound but that there is significant bonding in the Pt^{III}_2 complexes.[8] This increase in intermetallic bonding correlates with the shorter Pt(III)–Pt(III) distances found for $K_4[Pt_2(\mu\text{-}P_2O_5H_2)_4Cl_2]$ (2.695 (1) Å),[4] $(n\text{-}Bu_4N)_4[Pt_2(\mu\text{-}P_2O_5H_2)_4Br_2]$ (2.716 (1) Å), and $K_4[Pt_2(\mu\text{-}P_2O_5H_2)_4I_2]$ (2.754 (1) Å) than was found in $K_4[Pt_2(\mu\text{-}P_2O_5H_2)_4]\cdot 2H_2O$ (2.925 (1) Å). The Pt(III)–Pt(III) bond has a high trans influence, resulting in long Pt(III)–X (X = Cl, Br, I) distances.[9] In this paper we use halide replacement reactions to try to assess the influence of the intermetallic bond on the reactivity of the axial ligands in these diplatinum(III) complexes.

Experimental Section

Equipment. Infrared spectra were recorded (Nujol, KBr pellet) on a Perkin-Elmer 283B spectrophotometer. Far-infrared spectra were obtained as vaseline mulls on polyethylene with a Perkin-Elmer Hitachi FIS-3 spectrometer. Raman spectra were recorded on a ISA Jobin Yvon Ramanor HG2S spectrometer by using the 4880- and 5145-Å excitation wavelengths of an argon ion laser at 50 mW of power. Aqueous sample solutions for Raman spectroscopy were cooled in an ice bath and circulated through a glass capillary sample tube with a peristaltic pump. Raman spectra were enhanced by computer combination of repeated scans. Electronic spectra were recorded on Cary 14, Cary 219, and Hewlett-Packard Model 8451 A diode array spectrophotometers.

^{31}P NMR spectra were measured as deoxygenated D_2O solutions in 12-mm tubes on a Nicolet NT 200 FT spectrometer or in 10-mm tubes on a JEOL FX90 FT spectrometer. Typical pulse angles were 30° with an acquisition time of 0.8–4 s at 80.98 MHz for the NT 200. ^{195}Pt NMR spectra were measured on the NT 200 instrument by using 30° pulse angles and 0.2-s acquisition times. Spectra were measured at the ambient probe temperature (22 ± 1 °C) with use of an internal deuterium (D_2O) lock. ^{31}P shifts were recorded relative to external 85% H_3PO_4, and ^{195}Pt shifts were recorded relative to a 5.5 M H_2PtCl_6 solution in D_2O as standard reference. Chemical shifts are in parts per million with positive high-frequency shifts.

Electrochemical measurements were carried out on a PAR Model 170 electrochemical apparatus. Electrodes were purchased from Bioanalytical Systems, West Lafayette, IN, and solvents were N_2 purged prior to measurements. Photochemical experiments were carried out by using a 200-W Hg lamp (Illumination Industries) enclosed in an air-cooled housing (Ealing Corp.). Wavelength selection was by Schott sharp cutoff filters (WG 335 or WG 360). Quantum yield measurements were made on a SPEX fluorolog fluorimeter using the ferrioxalate actinometer. This instrument was chosen for these measurements because of the availability of a stable source of monochromated UV radiation (400-W xenon lamp).

Materials. K_2PtCl_4, K_2PtCl_6 and $H_2PtCl_6\cdot H_2O$ were purchased from Johnson Matthey Inc. and Engelhard Corp. Samples yielding $K_4[Pt_2(\mu\text{-}P_2O_5H_2)_4]\cdot 2H_2O$ of high purity in good yield were used without purification.[3] All other reagents were commercial samples and used as supplied. Water was purified by distillation in glass. Analyses were performed by Canadian Microanalytical Services, Vancouver, B.C., Canada.

Tetrapotassium Dichlorotetrakis(μ-pyrophosphito)diplatinate(III), $K_4[Pt_2(\mu\text{-}P_2O_5H_2)_4Cl_2]$. Chlorine gas was passed slowly through a deoxygenated aqueous solution of $K_4[Pt_2(\mu\text{-}P_2O_5H_2)_4]\cdot 2H_2O$ (0.5 g; 1.2 mmol) in water (~5 mL) for 20 min. The solution immediately changed color to yellow as the green emission from $K_4[Pt_2(\mu\text{-}P_2O_5H_2)_4]\cdot 2H_2O$ was lost. The water volume was reduced on a rotary evaporator, and the product precipitated as a bright yellow powder by the slow addition of ethanol or acetonitrile. The complex was washed with ethanol and dried in vacuo at ambient temperature; yield 60–70%. Anal. Calcd for $H_8Cl_2O_{20}P_8Pt_2K_4$: Cl, 5.9; P, 20.8. Found: Cl, 7.2; P, 19.5. The complex contains a small amount of K_2PtCl_6 as impurity that does not significantly affect the kinetics results. IR: ν(P=O) 1060 cm^{-1}; ν(P—O) 940 cm^{-1}; ν(Pt—Pt) 158 cm^{-1}; ν(Pt—Cl) 304 cm^{-1}. NMR: $\delta(^{31}P)$ 27.96 ($^1J(^{195}Pt-^{31}P)$ = 2086 Hz); $\delta(^{195}Pt)$ −4236. λ_{max}: 282 nm ($\epsilon = 5 \times 10^4$), 345 nm ($\epsilon = 7 \times 10^3$).

Tetrapotassium Dibromotetrakis(μ-pyrophosphito)diplatinate(III) Tetrahydrate, $K_4[Pt_4(\mu\text{-}P_2O_5H_2)_4Br_2]\cdot 4H_2O$. An excess of liquid bromine was added to a deoxygenated aqueous solution of $K_4[Pt_2(\mu\text{-}P_2O_5H_2)_4]\cdot 2H_2O$ (0.5 g; 1.2 mmol) in water (~5 mL), and the mixture was stirred for 45 min in air. The solution becomes orange in color very quickly after

(1) Abstracted in part from the Ph.D. Theses of M.K.D. and S.A.B., Washington State University, 1982 and 1985, respectively.

(2) (a) Tulane University. (b) Present address: Shell Development Corp., Houston, TX 77001.

(3) Sperline, R. P.; Dickson, M. K.; Roundhill, D. M. *J. Chem. Soc., Chem. Commun.* **1977**, 62–63. Alexander, K. A., Bryan, S. A.; Dickson, M. K.; Hedden, D.; Roundhill, D. M. *Inorg. Synth.* **1986**, *24*, 211–213.

(4) Filomena Dos Remedios Pinto, M. A.; Sadler, P. J.; Neidle, S.; Sanderson, M. R.; Subbiah, A.; Kuroda, R. *J. Chem. Soc., Chem. Commun.* **1980**, 13–15. Marsh, R. E.; Herbstein, F. H. *Acta Crystallogr. Sect. B: Struct. Sci.* **1983**, *B39*, 280–287. Che, C. M.; Herbstein, F. H.; Schaefer, W. P.; Marsh, R. E.; Gray, H. B. *J. Am. Chem. Soc.* **1983**, *105*, 4604–4607.

(5) Che, C. M.; Schaefer, W. P.; Gray, H. B.; Dickson, M. K.; Stein, P. B.; Roundhill, D. M. *J. Am. Chem. Soc.* **1982**, *104*, 4253–4255. Che, C.-M.; Butler, L. G.; Grunthaner, P. J.; Gray, H. B. *Inorg. Chem.* **1985**, *24*, 4662–4665. King, C.; Fronczek, F. R.; Roundhill, D. M. *J. Chem. Soc., Dalton Trans.*, in press.

(6) Mann, K. R.; Gordon, J. G., II; Gray, H. B. *J. Am. Chem. Soc.* **1975**, *97*, 3553–3555.

(7) Fordyce, W. A.; Brummer, J. G.; Crosby, G. A. *J. Am. Chem. Soc.* **1981**, *103*, 7061–7064. Che, C.-M.; Butler, L. G.; Gray, H. B. *J. Am. Chem. Soc.* **1981**, *103*, 7796–7797. Rice, S. F.; Gray, H. B. *J. Am. Chem. Soc.* **1983**, *105*, 4571–4575. Bar, L.; Gliemann, G. *Chem. Phys. Lett.* **1984**, *108*, 14–17. Markert, J. T.; Clements, D. P.; Corson, M. R.; Nagle, J. K. *Chem. Phys. Lett.* **1983**, *97*, 175–179. Parker, W. L.; Crosby, G. A. *Chem. Phys. Lett.* **1984**, *105*, 544–546. Shimizu, Y.; Tanaka, Y.; Azumi, T. *J. Phys. Chem.* **1984**, *88*, 2423–2425. Isci, H.; Mason, W. R. *Inorg. Chem.* **1985**, *24*, 1761–1765. Reisch, G. A.; Turner, W. A.; Corson, M. R.; Nagle, J. K. *Chem. Phys. Lett.* **1985**, *117*, 561–565. Alexander, K. A.; Stein, P.; Hedden, D. B.; Roundhill, D. M. *Polyhedron* **1983**, *2*, 1389–1392. Brummer, J. G.; Crosby, G. A. *Chem. Phys. Lett.* **1984**, *112*, 15–19. Roundhill, D. M. *Sol. Energy* **1986**, *36*, 297–299. Dickson, M. K.; Pettee, S. K.; Roundhill, D. M. *Anal. Chem.* **1981**, *53*, 2159–2160. Heuer, W. B.; Totten, M. D.; Rodman, G. S.; Hebert, E. J.; Tracy, H. J.; Nagle, J. K. *J. Am. Chem. Soc.* **1984**, *106*, 1163–1164. Stiegman, A. E.; Rice, S. F.; Gray, H. B.; Miskowski, V. M. *Inorg. Chem.* **1987**, *26*, 1112–1116.

(8) Stein, P.; Dickson, M. K.; Roundhill, D. M. *J. Am. Chem. Soc.* **1983**, *105*, 3489–3494. Che, C. M.; Butler, L. G.; Gray, H. B.; Crooks, R. M.; Woodruff, W. H. *J. Am. Chem. Soc.* **1983**, *105*, 5492–5494.

(9) Alexander, K. A.; Bryan, S. A.; Fronczek, F. R.; Fultz, W. C.; Rheingold, A. L.; Roundhill, D. M.; Stein, P.; Watkins, S. F. *Inorg. Chem.* **1985**, *24*, 2803–2808. Hedden, D.; Roundhill, D. M.; Walkinshaw, M. D. *Inorg. Chem.* **1985**, *24*, 3146–3150. Che, C.-M.; Mak, T. W.; Gray, H. B. *Inorg. Chem.* **1984**, *23*, 4386–4388.

bromine addition. Slow addition of ethanol yields an orange powder. The solid complex was washed with ethanol or methanol and dried in vacuo at ambient temperature; yield 70–80%. Anal. Calcd for $H_{16}Br_2O_{24}P_8Pt_2K_4$: Br, 11.8; P, 18.3. Found: Br, 11.2; P, 18.6. IR: ν(P=O) 1092 cm^{-1}; ν(P—O) 930 cm^{-1}; ν(Pt—Pt) 134 cm^{-1}; ν(Pt—Br) 224 cm^{-1}. NMR: $\delta(^{31}P)$ 24.01 ($^1J(^{195}Pt-^{31}P)$ = 2100 Hz); $\delta(^{195}Pt)$ −4544. λ_{max}: 305 nm ($\epsilon = 5.5 \times 10^4$), 350 nm ($\epsilon = 12 \times 10^3$).

Tetrapotassium Diiodotetrakis(μ-pyrophosphito)diplatinate(III), $K_4[Pt_2(\mu-P_2O_5H_2)_4I_2]$. Excess iodine was added to a deoxygenated aqueous solution of $K_4[Pt_2(\mu-P_2O_5H_2)_4]\cdot 2H_2O$ (0.5 g; 1.2 mmol) in water (~5 mL) to produce a deep red-brown color. Slow addition of ethanol, methanol, or acetonitrile gave a red brown powder, which was dried in vacuo at ambient temperature; yield 70–75%. Anal. Calcd for $H_8I_2O_{20}P_8Pt_2K_4$: I, 18.4; P, 18.0. Found: I, 18.6; P, 17.7. IR: ν(P=O) 1090 cm^{-1}, ν(P—O) 920 cm^{-1}; ν(Pt—Pt) 110 cm^{-1}, ν(Pt—I) 195 cm^{-1}. NMR: $\delta(^{31}P)$ 18.01 ($^1J(^{195}Pt-^{31}P)$ = 2139 Hz); $\delta(^{195}Pt)$ −5103. λ_{max}: 331 nm ($\epsilon = 4 \times 10^4$), 438 nm ($\epsilon = 17 \times 10^3$).

Tetrapotassium Chloroiodotetrakis(μ-pyrophosphito)diplatinate(III), $K_4[Pt_2(\mu-P_2O_5H_2)_4ICl]$. To a solution of $K_4[Pt_2(\mu-P_2O_5H_2)_4]$ (3.7×10^{-5} M) in HCl (ca. 2 mL of 0.1 M) was added solid iodine (~1 mg). After mixing, the solution contained the complex $Pt_2(\mu-P_2O_5H_2)_4ClI^{4-}$ (λ_{max} = 313 nm ($\epsilon = 4.1 \times 10^4$ cm^{-1} M^{-1}), 430 nm ($\epsilon = 1.0 \times 10^4$ cm^{-1} M^{-1})). ^{31}P NMR: δ 26.47 ($^1J(^{195}Pt-^{31}P)$ = 2236 Hz), 19.46 ($^1J(^{195}Pt-^{31}P)$ = 2175 Hz). Attempted isolation in the solid state yielded a mixture of $Pt_2(\mu-P_2O_5H_2)_4Cl_2^{4-}$ and $Pt_2(\mu-P_2O_5H_2)_4I_2^{4-}$.

Tetrapotassium Chlorobromotetrakis(μ-pyrophosphito)diplatinate(III), $K_4[Pt_2(\mu-P_2O_5H_2)_4BrCl]$. To a solution of $K_4[Pt_2(\mu-P_2O_5H_2)_4]$ (2×10^{-5} M) in HCl (excess of 0.1 M) was added liquid bromine (ca. 0.1 mL). After nitrogen was passed through the solution to remove excess bromine, the solution contained $Pt_2(\mu-P_2O_5H_2)_4BrCl^{4-}$ (λ_{max} = 298 ($\epsilon = 5.6 \times 10^4$ cm^{-1} M^{-1}), 388 nm ($\epsilon = 3.1 \times 10^4$ cm^{-1} M^{-1})). ^{31}P NMR: δ 27.42 ($^1J(^{195}Pt-^{31}P)$ = 2151 Hz), 24.38 ($^1J(^{195}Pt-^{31}P)$ = 2153 Hz). Concentration of the solution led to disproportionation into $Pt_2(\mu-P_2O_5H_2)_4Br_2^{4-}$ and $Pt_2(\mu-P_2O_5H_2)_4Cl_2^{4-}$.

Tetrapotassium Bromoiodotetrakis(μ-pyrophosphito)diplatinate(III), $K_4[Pt_2(\mu-P_2O_5H_2)_4BrI]$. To a solution of $K_4[Pt_2(\mu-P_2O_5H_2)_4]$ (ca. 2.4×10^{-5} M) in phosphoric acid (pH 1) and potassium bromide (0.1 M) was added solid iodine (1–2 mg). The solution contained $Pt_2(\mu-P_2O_5H_2)_4BrI^{4-}$ (λ_{max} = 316 nm ($\epsilon = 5.2 \times 10^4$ cm^{-1} M^{-1}), 350 nm (shoulder). Concentration of the solution led to disproportionation into $Pt_2(\mu-P_2O_5H_2)_4Br_2^{4-}$ and $Pt_2(\mu-P_2O_5H_2)_4I_2^{4-}$.

Kinetic Measurements. Solutions for kinetic measurements were prepared from commercial grade inorganic chemicals, and water having a pH of 7 prepared by distillation in a glass apparatus. Solutions were prepared in volumetric flasks, which were carefully cleaned periodically with nitric acid and water. Cells for the UV–vis spectrometer were matched 1-cm path length quartz cells, and these were cleaned periodically by the same procedure as that used for the volumetric flasks.

Phosphate buffer solutions[10] (pH 6.0; KH_2PO_4–K_2HPO_4) were prepared by using reagent grade chemicals. The solution pH was verified against commercial buffer solutions with a Corning Model 125 pH meter. Solutions were initially prepared of ionic strength 0.100 M. Reagent grade sodium perchlorate was added where necessary to adjust the ionic strength.

All kinetic measurements were made at 25 ± 0.3 °C in a quartz 1-cm path length cell by using the Hewlett-Packard Model 8451 Å spectrophotometer. The reagents $K_4[Pt_2(\mu-P_2O_5H_2)_4X_2]$ (X = Cl, Br, I) were added in measured quantities as solids or solutions to the buffer solution (2–3 mL) in the cell. In all cases the purity of the complexes was checked by a combination of UV–vis and ^{31}P NMR spectroscopy. The concentration range for measurement was 1.45×10^{-5} to 6.30×10^{-5} M. The catalyst $K_4[Pt_2(\mu-P_2O_5H_2)_4]\cdot 2H_2O$ was added as a solid or as a solution, and its concentration was measured spectrophotometrically (λ_{max} 367 nm, ϵ = 32 500 cm^{-1} M^{-1}). Sodium chloride, if required, was added with a Pipetman (Rainin Instrument Co., Inc.) from a stock solution. The reactions were initiated by the addition of an appropriate quantity of standardized potassium iodide or potassium bromide or by the addition of a mixed potassium iodide–iodine solution. Transfer was by Pipetman from stock solutions of constant ionic strength buffered to pH 6. The complexes $K_4[Pt_2(\mu-P_2O_5H_2)_4X_2]$ (X = Cl, Br, I) in aqueous solution obey Beer's law, and concentration changes have been monitored for both the disappearance of reactant complex and the formation of product complex.

Photochemical Measurements. Quantum yield measurements with the SPEX Fluorolog fluorimeter and the potassium ferrioxalate actinometer were carried out by using excitation wavelength of 286, 310, and 338 nm. Typical measurements were made in buffered aqueous solutions (pH 6; 0.10 M ionic strength). Comparative light and dark measurements were made with identical solutions and quartz UV cells. During photolysis the exposed solution was continuously stirred. Both cells were thermostated at 25 ± 0.3 °C. Reaction progress in each cell was measured spectrophotometrically by using the Hewlett-Packard Model 8451A spectrophotometer. The contribution from the blank (dark) reaction was subtracted from that of the photolyzed reaction.

Potentiometric Titrations. The potentiometric titration of a solution of $Pt_2(\mu-P_2O_5H_2)_4^{4-}$ was performed with a standard ceric solution by using a platinum indicator electrode and a SCE reference. A solution of $(NH_4)_2Ce(NO_3)_6$ (ca. 0.01 M) in aqueous H_2SO_4 was prepared and standardized against sodium oxalate by potentiometric titration with a platinum indicator and a SCE reference electrode system. $K_4[Pt_2(\mu-P_2O_5H_2)_4]\cdot 2H_2O$ (19.7 mg, 17 μmol) in ca. 4 mL of 0.1 M HCl solution was titrated with the standard ceric solution. Millivolt and pH measurements were made by using platinum wire electrodes against an SCE electrode (Corning) or against a semimicro combination electrode (Corning) on a Corning Model 125 pH meter.

Acid–Base Titrations. A Brinkman Metrohm Combititrator 3D system equipped with a Multi-Dosmat E415 dispenser, an Impulsomat E473 chart drive with internal chart recorder, and an E512 pH meter with a glass pH electrode (Metrohm Ag 9100 Herisau) were used for each titration. The pH electrode was standardized against a commercial buffer (pH 7.00 ± 0.01, Curtin Matheson Scientific Inc.) Each sample, $K_4[Pt_2(\mu-P_2O_5H_2)_4]\cdot 2H_2O$ and $K_4[Pt_2(\mu-P_2O_5H_2)_4X_2]$ (X = Cl, Br, I) (≈26-36 μmol) was dissolved in deionized water (5 mL), and sufficient HCl (0.10 M) was added to lower the pH to the 1.8–2.2 range. Each solution was titrated with NaOH solution (1.5×10^{-2} M) until a solution pH in the range of 12 was reached.

Calorimetry. Calorimetric titrations were performed on a modified isothermal titration microcalorimeter (Tronac Inc., Model 550) at a constant temperature (25.000 ± 0.005 °C). A potassium iodide solution (0.5110 M) was titrated into the reaction vessel containing an aqueous solution of $K_4[Pt_2(\mu-P_2O_5H_2)_4]\cdot 2H_2O$ (50.00 mL of 4.704×10^{-3} M). The solution in the vessel was purged with nitrogen prior to the titration. Heat data were corrected for the heat of dilution of KI. A similar correction for the platinum complex was found to be unnecessary. The corrected heat data were fit to a model that assumed a 1:1 interaction between $Pt_2(\mu-P_2O_5H_2)_4^{4-}$ and I^-. The equilibrium constant and enthalpy of reaction were the only adjustable parameters in this least-squares computer fit. The entropy of reaction was calculated from the obtained ΔG value.

Results and Discussion

Synthesis and Solution Stability of μ-Pyrophosphito Diplatinum Complexes. The binuclear platinum(II) and platinum(III) complexes $K_4[Pt_2(\mu-P_2O_5H_2)_4]\cdot 2H_2O$ and $K_4[Pt_2(\mu-P_2O_5H_2)_4X_2]$ (X = Cl, Br, I) are air-stable solids that are soluble in water but insoluble in organic solvents. Aqueous solutions are acidic, and solutions of the complexes have their highest stability in the 0–6.5 range of pH. Above pH 7, solutions of $Pt_2(\mu-P_2O_5H_2)_4^{4-}$ rapidly decompose to give platinum metal. Solutions of $K_4[Pt_2(\mu-P_2O_5H_2)_4]$ that are maintained at a pH in the 1–6.5 range undergo hydrolysis over a period of 1–2 days to give $Pt[(OP(OH)_2)_4H_2]$.[11] The hydrolytic reaction (eq 1) can be followed by ^{31}P NMR

$$Pt_2(\mu-P_2O_5H_2)_4^{4-} + 8H_2O \rightarrow 2Pt[(OP(OH)_2)_4H_2] + 4OH^- \quad (1)$$

spectroscopy, when the peak due to $Pt_2(\mu-P_2O_5H_2)_4^{4-}$, centered at δ 66.5, is progressively replaced by the resonance at δ 83.1 for $Pt[(OP(OH)_2)_4H_2]$.[12] This hydrolysis is a reversal of the condensation reaction used in the synthesis of $Pt_2(\mu-P_2O_5H_2)_4^{4-}$, and the reaction pathway most likely involves nucleophilic cleavage by water or hydroxide ion of the bridging pyrophosphito (POP) moiety.

Reaction Chemistry. Halogen addition to $Pt_2(\mu-P_2O_5H_2)_4^{4-}$ gives $Pt_2(\mu-P_2O_5H_2)_4X_2^{4-}$ (X = Cl, Br, I), where the halide ligands are coordinated in the axial positions (eq 2).[5,9] Over the pH range

$$Pt_2(\mu-P_2O_5H_2)_4^{4-} + X_2 \rightarrow Pt_2(\mu-P_2O_5H_2)_4X_2^{4-} \quad (2)$$

of 1–6.5, aqueous solutions of $Pt_2(\mu-P_2O_5H_2)_4X_2^{4-}$ show *no*

(10) Boyd, W. C. *J. Biol. Chem.* **1965**, *240*, 4097–4098.

(11) Troitskaya, A. D. *Russ. J. Inorg. Chem.* (*Engl. Transl.*) **1961**, *6*, 585–586.

(12) Dickson, M. K. Ph.D. Thesis, Washington State University, 1982.

Table I. pK_a Values for the Complexes $Pt_2(\mu\text{-}P_2O_5H_2)_4^{4-}$ and $Pt_2(\mu\text{-}P_2O_5H_2)_4X_2^{4-}$ (X = Cl, Br, I)

complex	pK_1	pK_2	pK_3
$Pt_2(\mu\text{-}P_2O_5H_2)_4^{4-}$	2.24	6.75	
$Pt_2(\mu\text{-}P_2O_5H_2)_4Cl_2^{4-}$	2.55	4.72	6.72
$Pt_2(\mu\text{-}P_2O_5H_2)_4Br_2^{4-}$	2.62	5.10	7.21
$Pt_2(\mu\text{-}P_2O_5H_2)_4I_2^{4-}$	2.68	5.56	7.80

tendency to undergo aquation of the axial halide ligands. These dihalo complexes can also be prepared by treating a mixture of $Pt_2(\mu\text{-}P_2O_5H_2)_4^{4-}$ and halide ion with one-electron oxidants such as $IrCl_6^{2-}$ and Ce^{4+} (eq 3).[13] Alternatively an electrochemical

$$Pt_2(\mu\text{-}P_2O_5H_2)_4^{4-} \xrightarrow{-e^-,\,X^-} Pt_2(\mu\text{-}P_2O_5H_2)_4X^{4-} \xrightarrow{-e^-,\,X^-} Pt_2(\mu\text{-}P_2O_5H_2)_4X_2^{4-} \quad (3)$$

method can be used; oxidation of a solution of $Pt_2(\mu\text{-}P_2O_5H_2)_4^{4-}$ and X^- (X = Cl, Br, I) at pH 1–2 with a Pt-gauze electrode at +0.8 V vs Ag/AgCl gives $Pt_2(\mu\text{-}P_2O_5H_2)_4X_2^{4-}$. At 0.0 V or by chemical use of H_3PO_2, Na_2SO_3, $Na_2S_2O_3$, ascorbic acid, or Zn/Hg, the reaction can be reversed to give $Pt_2(\mu\text{-}P_2O_5H_2)_4^{4-}$.[13,14] If $Pt_2(\mu\text{-}P_2O_5H_2)_4^{4-}$ is chemically or electrochemically oxidized in the absence of added halide ion, the diplatinum(III) complex $Pt_2(\mu\text{-}P_2O_5H_2)_4(H_2O)_2^{2-}$ is formed (eq 4). This complex is

$$Pt_2(\mu\text{-}P_2O_5H_2)_4^{4-} \xrightarrow{-2e^-} Pt_2(\mu\text{-}P_2O_5H_2)_4(H_2O)_2^{2-} \quad (4)$$

characterized by an absorption band at 248 nm. This anion is unstable in aqueous solutions, and the solution begins to deposit metallic platinum after standing for a few minutes at ambient temperature, even under acidic conditions (eq 5).

$$Pt_2(\mu\text{-}P_2O_5H_2)_4(H_2O)_2^{2-} + 5H_2O \rightarrow 2Pt + 5H_2PO_3^- + 3H_2PO_4^- + 6H^+ \quad (5)$$

Solutions of the mixed-halo complexes $Pt_2(\mu\text{-}P_2O_5H_2)_4XY^{4-}$ can be prepared by treating a mixture of $Pt_2(\mu\text{-}P_2O_5H_2)_4^{4-}$ and halide X^- with a small quantity of the halogen Y_2 (eq 6). Not

$$Pt_2(\mu\text{-}P_2O_5H_2)_4^{4-} + X^- + Y_2 \xrightarrow{\text{pH 1}} Pt_2(\mu\text{-}P_2O_5H_2)_4XY^{4-} + Y^- \quad (6)$$

all combinations of X^- and Y_2 are possible; the reaction will only give the mixed product XY when X_2 is a stronger oxidant than is Y_2. The reaction *must* be carried out at low pH, or the initially formed complex $Pt_2(\mu\text{-}P_2O_5H_2)_4XY^{4-}$ will undergo subsequent substitution by excess X^- to give $Pt_2(\mu\text{-}P_2O_5H_2)_4X_2^{4-}$. An alternative route to prepare these mixed-dihalo complexes is to treat the diplatinum(III) complex $Pt_2(\mu\text{-}P_2O_5H_2)_4X_2^{4-}$ with a small quantity of halogen Y_2. Excess of the halogen gives $Pt_2(\mu\text{-}P_2O_5H_2)_4Y_2^{4-}$ (eq 7).[13] All these changes can be followed by UV-vis, Raman, or by ^{31}P NMR spectroscopy.

$$Pt_2(\mu\text{-}P_2O_5H_2)_4X_2^{4-} \xrightarrow{Y_2} Pt_2(\mu\text{-}P_2O_5H_2)_4XY^{4-} \xrightarrow{Y_2} Pt_2(\mu\text{-}P_2O_5H_2)_4Y_2^{4-} \quad (7)$$

Effect of pH on the Solution Species. Before we can address the questions of kinetics and mechanism, we must first identify the species present in solution under different pH conditions. We have carried out pH titrations after the initial addition of a strong acid, and find that $Pt_2(\mu\text{-}P_2O_5H_2)_4^{4-}$ is a dibasic acid and that the complexes $Pt_2(\mu\text{-}P_2O_5H_2)_4X_2^{4-}$ are tribasic acids. The data are collected together in Table I. These data show that the first pK (pK_1) is in the region of 2.2–2.7 and that pK_2 for $Pt_2(\mu\text{-}P_2O_5H_2)_4^{4-}$ is at 6.75. For the Pt^{III}_2 complexes $Pt_2(\mu\text{-}P_2O_5H_2)_4X_2^{4-}$ we observe pK_2 and pK_3 in the respective ranges of 5 and 7. These deprotonations from $Pt_2(\mu\text{-}P_2O_5H_2)_4^{4-}$ and $Pt_2(\mu\text{-}P_2O_5H_2)_4X_2^{4-}$ are shown in eq 8 and 9. No significant spectral changes λ_{max}

$$Pt_2(\mu\text{-}P_2O_5H_2)_4^{4-} \underset{H^+}{\overset{OH^-}{\rightleftharpoons}} Pt_2(\mu\text{-}P_2O_5H_2)_3(\mu\text{-}P_2O_5H)^{5-} \underset{H^+}{\overset{OH^-}{\rightleftharpoons}} Pt_2(\mu\text{-}P_2O_5H_2)_2(\mu\text{-}P_2O_5H)_2^{6-} \quad (8)$$

$$Pt_2(\mu\text{-}P_2O_5H_2)_4X_2^{4-} \underset{H^+}{\overset{OH^-}{\rightleftharpoons}} Pt_2(\mu\text{-}P_2O_5H_2)_3(\mu\text{-}P_2O_5H)X_2^{5-} \underset{H^+}{\overset{OH^-}{\rightleftharpoons}} Pt_2(\mu\text{-}P_2O_5H_2)(\mu\text{-}P_2O_5H)_2X_2^{6-} \underset{H^+}{\overset{OH^-}{\rightleftharpoons}} Pt_2(\mu\text{-}P_2O_5H_2)(\mu\text{-}P_2O_5H)_3X_2^{7-} \quad (9)$$

are observed with variations in pH, suggesting that the electron density differences in the variable-charged species are primarily located at the ligand periphery rather than at the central bimetallic core.

Rate Data. All rate data were collected at a constant temperature of 25 ± 0.3 °C. All solutions were maintained at a pH of 6 with a phosphate buffer. Where necessary, sodium perchlorate was added to maintain constant ionic strength. The complexes all obey Beer's law, and we have collected concentration against time data by collecting intensity data at λ_{max} for both the reactant and product against elapsed time. The UV–vis spectrometer is preprogrammed to measure and store intensity and time data. The chosen time interval depends on the particular reaction being studied, and the intensity data are collected for the chosen λ_{max} values. The instrument resolution is 2 nm. In a typical reaction, some 100–120 absorbance data points against time are recorded and stored. A plot of ln $(A_t - A_\infty)$ against time is linear for data collected to greater than 95% of the reaction completion. The A_∞ value is experimentally determined and then adjusted to give the best linear least squares fit to the ln $(A_t - A_\infty)$ against time data. An analogous data treatment method is used for all reactions. The substitution reactions are selectively axial to give a single product. Isosbestic points are observed in all cases. We observe *no* intermediate formation of $Pt_2(\mu\text{-}P_2O_5H_2)_4XY^{4-}$. From the linearity of the ln $(A_t - A_\infty)$ vs time plots, we conclude that the reactions are first order in $Pt_2(\mu\text{-}P_2O_5H_2)_4X_2^{4-}$, and we have evaluated all the k_{obsd} values. All measurements have been carried out under thermal dark conditions in the enclosed spectrometer cell compartment. The operation of the diode array spectrometer ensures the absence of photochemical reaction, except for the short duration time of the flash for the spectral measurement.

In the absence of added $Pt_2(\mu\text{-}P_2O_5H_2)_4^{4-}$, plots of ln $(A_t - A_\infty)$ against time for the reaction of $Pt_2(\mu\text{-}P_2O_5H_2)_4X_2^{4-}$ with Y^- are only approximately linear, and closer inspection shows the plots to be actually S shaped. Such plots are characteristic of autocatalytic reactions. This curvature in these plots is removed and the substitution rate increases, when the diplatinum(II) complex $Pt_2(\mu\text{-}P_2O_5H_2)_4^{4-}$ is added to the reaction mixture. Thus it is apparent that this complex is a catalyst for the halide substitution reaction and that even when not added initially, it is formed in small amounts by the reductive elimination of halogen from $Pt_2(\mu\text{-}P_2O_5H_2)_4X_2^{4-}$.

The experimental rate data show that the rate of substitution of the halide ion X^- in $Pt_2(\mu\text{-}P_2O_5H_2)_4X_2^{4-}$ by Y^- is dependent on $Pt_2(\mu\text{-}P_2O_5H_2)_4X_2^{4-}$, $Pt_2(\mu\text{-}P_2O_5H_2)_4^{4-}$, and Y^-. We have measured the reaction rates where X = Cl, Y = I; X = Cl, Y = Br; and X = Br, Y = I. The most detailed study has been made for the reaction of $Pt_2(\mu\text{-}P_2O_5H_2)_4Cl_2^{4-}$ with iodide ion. We will present evidence to argue that at least three pathways are operable in the substitution mechanism. The predominant pathway is one that is catalyzed by $Pt_2(\mu\text{-}P_2O_5H_2)_4^{4-}$ (eq 10).[15] A second slower

$$Pt_2(\mu\text{-}P_2O_5H_2)_4X_2^{4-} + Pt_2(\mu\text{-}P_2O_5H_2)_4^{4-} + 2Y^- \rightarrow Pt_2(\mu\text{-}P_2O_5H_2)_4Y_2^{4-} + Pt_2(\mu\text{-}P_2O_5H_2)_4^{4-} + 2X^- \quad (10)$$

(13) Bryan, S. A.; Dickson, M. K.; Roundhill, D. M. *J. Am. Chem. Soc.* **1984**, *106*, 1882–1883.
(14) Bryan, S. A.; Schmehl, R. H.; Roundhill, D. M. *J. Am. Chem. Soc.* **1986**, *108*, 5408–5412.
(15) Mason, W. R. *Coord. Chem. Rev.* **1972**, *7*, 241–255.

Scheme I.[a] Generalized Mechanistic Sequences for the Reaction of $Pt_2(\mu\text{-}P_2O_5H_2)_4X_2^{4-}$ with Y^-

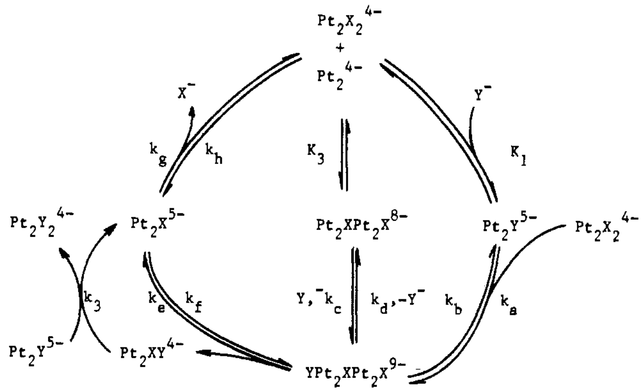

[a]The equatorial $\mu\text{-}P_2O_5H_2$ ligands are omitted for clarity.

Table II. k_{obsd} vs $[I^-]$ for the Reaction of $Pt_2(\mu\text{-}P_2O_5H_2)_4Cl_2^{4-}$ with I^- [a]

k_{obsd}, s^{-1}	$[I^-]$, M	k_{obsd}, s^{-1}	$[I^-]$, M
7.13 (±0.23) × 10^{-3}	1.56 × 10^{-5}	4.45 (±0.14) × 10^{-2}	6.25 × 10^{-4}
1.38 (±0.11) × 10^{-2}	3.91 × 10^{-5}	4.85 (±0.15) × 10^{-2}	1.25 × 10^{-3}
2.12 (±0.03) × 10^{-2}	7.81 × 10^{-5}	4.87 (±0.20) × 10^{-2}	1.88 × 10^{-3}
3.07 (±0.09) × 10^{-2}	1.56 × 10^{-4}	5.35 (±0.25) × 10^{-2}	2.50 × 10^{-3}
3.90 (±0.12) × 10^{-2}	3.13 × 10^{-4}		

[a] $[Pt_2(\mu\text{-}P_2O_5H_2)_4^{4-}]$ = 2.36 × 10^{-5} M; $[Pt_2(\mu\text{-}P_2O_5H_2)_4Cl_2^{4-}]_0$ = 5.48 × 10^{-6} M; μ = 0.110 M at pH 6.0.

pathway is the *direct* replacement of X by Y^- in a reductive-elimination–oxidative-addition (REOA) sequence (eq 11).[16] The

$$Pt_2(\mu\text{-}P_2O_5H_2)_4X_2^{4-} + 2Y^- \rightarrow Pt_2(\mu\text{-}P_2O_5H_2)_4Y_2^{4-} + 2X^- \quad (11)$$

$$Pt_2(\mu\text{-}P_2O_5H_2)_4X_2^{4-} + H_2O \rightarrow Pt_2(\mu\text{-}P_2O_5H_2)_4X(H_2O)^{3-} + X^- \xrightarrow{Y^-} Pt_2(\mu\text{-}P_2O_5H_2)_4XY^{4-} + X^- \quad (12)$$

third, and slowest, pathway is a simple dissociative mechanism (eq 12). Since there are small, but significant, differences in the reactions between individual complexes $Pt_2(\mu\text{-}P_2O_5H_2)_4X_2^{4-}$ with Y^-, we will treat each case separately.

Thermal Reaction Pathways. (a) Catalyzed Pathways. From our experimental data, it is clear that these substitution reactions of X^- in $Pt_2(\mu\text{-}P_2O_5H_2)_4X_2^{4-}$ by Y^- are catalyzed by $Pt_2(\mu\text{-}P_2O_5H_2)_4^{4-}$. Three replacement reactions have been investigated: the reaction between $Pt_2(\mu\text{-}P_2O_5H_2)_4Cl_2^{4-}$ and both Br^- and I^- and the reaction of I^- with $Pt_2(\mu\text{-}P_2O_5H_2)_4Br_2^{4-}$. The reaction between $Pt_2(\mu\text{-}P_2O_5H_2)_4Cl_2^{4-}$ and I^- has been studied in the most detail, but all three substitution reactions show the same *general* features, along with differences in *specific* details in each reaction. Overall the substitution mechanisms can be explained on the basis of the general set of reactions shown in Scheme I.[17] In all cases we define K_n as k_n/k_{-n}.

In order to maintain simplicity, we designate the bridging ligand as $\mu\text{-}P_2O_5H_2^{2-}$ in all the complexes and intermediates. We recognize, however, that this is technically not correct in all cases. The difference in pK_2 values between $Pt_2(\mu\text{-}P_2O_5H_2)_4^{4-}$ and

(16) Peloso, A. *Coord. Chem. Rev.* **1973**, *10*, 123–181. Poë, A. J.; Vaughan, D. H. *J. Am. Chem. Soc.* **1970**, *92*, 7537–7542.

(17) The kinetic analysis has been simplified by making the following combinations. Combining k_a/k_b, k_e/k_f, and k_g/k_h gives

$$Pt_2(\mu\text{-}P_2O_5H_2)_4Y^{5-} + Pt_2(\mu\text{-}P_2O_5H_2)_4X_2^{4-} \underset{k_{-2}}{\overset{k_2}{\rightleftharpoons}} Pt_2(\mu\text{-}P_2O_5H_2)_4XY^{4-} + Pt_2(\mu\text{-}P_2O_5H_2)_4^{4-} + X^-$$

Combining k_c/k_d, k_e/k_f, and k_g/k_h gives

$$Pt_2(\mu\text{-}P_2O_5H_2)_4XPt_2(\mu\text{-}P_2O_5H_2)_4X^{8-} + Y^- \xrightarrow{k_4} Pt_2(\mu\text{-}P_2O_5H_2)_4XY^{4-} + Pt_2(\mu\text{-}P_2O_5H_2)_4^{4-} + X^-$$

Table III. k_{obsd} vs $[Cl^-]$ for the Reaction of $Pt_2(\mu\text{-}P_2O_5H_2)_4Cl_2^{4-}$ with I^- [a]

k_{obsd}, s^{-1}	$10[Cl^-]$, M	k_{obsd}, s^{-1}	$10[Cl^-]$, M
1.74 × 10^{-1}	0.817	1.00 × 10^{-1}	3.54
1.29 × 10^{-1}	1.73	8.44 × 10^{-2}	4.90
1.22 × 10^{-1}	2.18	7.71 × 10^{-2}	6.26
1.12 × 10^{-1}	2.45	6.81 × 10^{-2}	6.95
1.22 × 10^{-1}	2.86	5.19 × 10^{-2}	8.99

[a] $[I^-]_0$, $[Pt_2(\mu\text{-}P_2O_5H_2)_4^{4-}]_0$, and $[Pt_2(\mu\text{-}P_2O_5H_2)_4Cl_2^{4-}]_0$ are 23 × 10^{-3}, 5.39 × 10^{-6}, and 3.0 × 10^{-6} M, respectively; μ = 1.00 M at pH 6.0. Errors in k_{obsd} values were estimated at approximately 10% based on errors in A_∞.

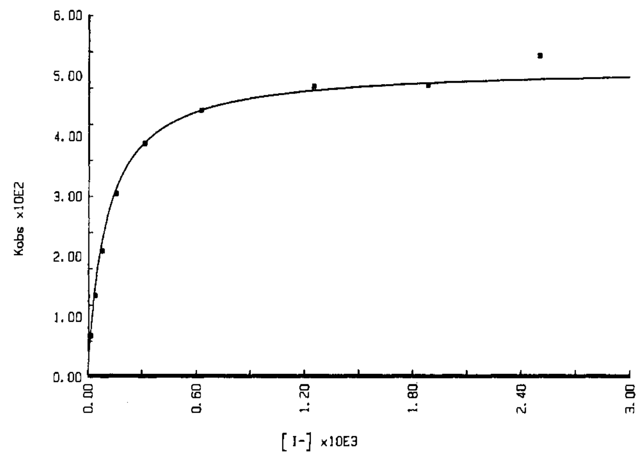

Figure 1. Plot of k_{obsd} against $[I^-]$ for the reaction of $Pt_2(\mu\text{-}P_2O_5H_2)_4Cl_2^{4-}$ with iodide with added $Pt_2(\mu\text{-}P_2O_5H_2)_4^{4-}$.

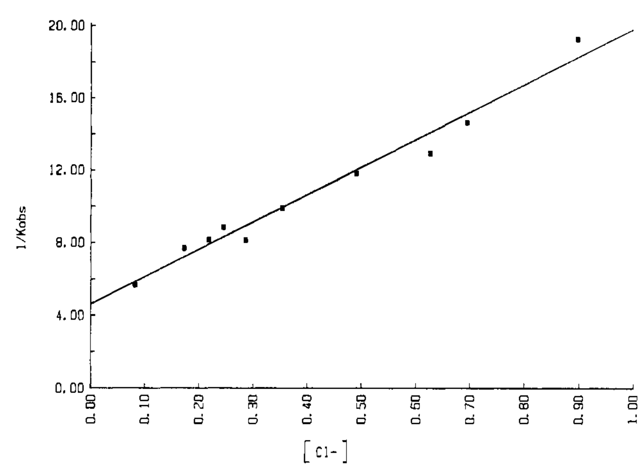

Figure 2. Plot of $1/k_{obsd}$ against $[Cl^-]$ for the reaction of $Pt_2(\mu\text{-}P_2O_5H_2)_4Cl_2^{4-}$ with iodide and $Pt_2(\mu\text{-}P_2O_5H_2)_4^{4-}$.

$Pt_2(\mu\text{-}P_2O_5H_2)_4X_2^{4-}$ makes it apparent that at pH 6 there is a charge difference between these complexes. This difference is especially significant when one realizes that in any platinum(II)-catalyzed substitution reaction there is metal center interchange in any single substitution step. We make the reasonable assumption that these proton-transfer steps are very rapid compared to the catalyzed halide-substitution reaction and that our constant ionic strength conditions attenuates charge effects endemic to these processes. It is very unlikely that the iodide ion in $Pt_2(\mu\text{-}P_2O_5H_2)_4ClI^{4-}$ exerts an extremely high trans effect through the Pt–Pt bond. There is no precedence for such a proposal, and indeed our own kinetic studies on the μ-hydrogen phosphato diplatinum(III) complexes show that there is no unexpectedly large trans effect through the intermetallic bond.[18]

In the reaction of $Pt_2(\mu\text{-}P_2O_5H_2)_4Cl_2^{4-}$ with I^-, the rate of substitution is directly proportional to the concentration of $Pt_2(\mu\text{-}P_2O_5H_2)_4^{4-}$. The rate dependence on added iodide ion is more complicated, and the k_{obsd} values are shown in Tables II and III. At low iodide concentration the rate is approximately first order in [I$^-$], but at higher added amounts k_{obsd} becomes independent of [I$^-$] (Figure 1).

The kinetic data can be fitted to the respective equations $k_{obsd} = a[I^-]/(1 + b[I^-])$, and $1/k_{obsd} = 1/a[I^-] + b/a$. These data from Table II have then been treated by Scatchard's method[19] in order to give equal weight to each piece of data. The respective values of a and b are found to be 500 M^{-1} s^{-1} and 9.8×10^3 M^{-1}.

In Table III we show the data for k_{obsd} against [Cl$^-$], which verify that the substitution reaction is inhibited by added chloride ion. These data can be fitted to the expression $1/k_{obsd} = r/p[Cl^-] + q/p$ (Figure 2). Using a least-squares fit, we evaluate r/p and q/p as 15.1 M^{-1}/s and 4.6 s, respectively. These experimental data can be fit to a mechanism where the predominant reactions are those shown in Scheme I (X = Cl, Y = I). Combining steps gives the rate law

$$\text{rate} = k_{obsd}[Pt_2(\mu\text{-}P_2O_5H_2)_4Cl_2^{4-}]$$

where

$$k_{obsd} = \frac{k_2k_3K_1^2[I^-]^2([Pt_2(\mu\text{-}P_2O_5H_2)_4^{4-}]/(1 + K_1[I^-]))}{k_{-2}[Cl^-] + k_3K_1[I^-]}$$

where the k_a/k_b, k_e/k_f, and k_g/k_h steps are combined to give a single k_2/k_{-2} step. We experimentally find the following values: $K_1 = 9.8$ (8) $\times 10^3$ M^{-1}, $k_2 = 2.2$ (5) $\times 10^3$ M^{-1} s^{-1}, and $k_{-2}/k_3 = 39.6$ (9) M^{-1} for the rate and equilibrium constants. An interesting result from this analysis is the large value found for K_1.

Additional support for the association between $Pt_2(\mu\text{-}P_2O_5H_2)_4^{4-}$ and I$^-$, comes from four separate experiments. Upon addition of I$^-$ to aqueous solutions of $Pt_2(\mu\text{-}P_2O_5H_2)_4^{4-}$, we observe no change in the λ_{max} position at 368 nm. Careful inspection of the spectra obtained with increasing amounts of added I$^-$ show, however, a progressive broadening of the 368-nm absorption band to lower wavelength when the solution of pure $Pt_2(\mu\text{-}P_2O_5H_2)_4^{4-}$ is used as reference. A more definitive change is observed in the ^{195}Pt NMR spectrum of the complex. Upon addition of I$^-$ to aqueous solutions of $Pt_2(\mu\text{-}P_2O_5H_2)_4^{4-}$ there is a progressive downfield shift in the chemical shift δ from −5127 to −5076. At the highest concentration of I$^-$, we find that ^1J(Pt–P) = 3094 Hz. This coupling constant value represents a slight increase from that of 3064 Hz found in $Pt_2(\mu\text{-}P_2O_5H_2)_4^{4-}$. This shift direction verifies that the upfield change in the chemical shift is *not* caused by the formation of $Pt_2(\mu\text{-}P_2O_5H_2)_4I_2^{4-}$, for which ^1J(Pt–P) = 2139 Hz. Third, adding I$^-$ to aqueous solutions of $Pt_2(\mu\text{-}P_2O_5H_2)_4^{4-}$ results in a quenching of the triplet emission at 514 nm ($k = 2 \times 10^7$ M^{-1} s^{-1}). Since emission quenching in this complex occurs by an inner-sphere pathway, we can conclude that I$^-$ coordinates to the axial site in the triplet excited state $Pt_2(\mu\text{-}P_2O_5H_2)_4^{4-*}$. Fourth, we have measured both K_1 and the values of ΔH and ΔS by calorimetry. Using aqueous solutions of $K_4[Pt_2(\mu\text{-}P_2O_5H_2)_4]$ and KI, we obtained the respective values of 115 (1) M^{-1}, −1.13 (1) kcal mol^{-1}, and 5.63 (6) cal mol^{-1} K^{-1} for K_1, ΔH, and ΔS at 25.000 (5) °C. This value of K_1 confirms the strong association between $Pt_2(\mu\text{-}P_2O_5H_2)_4^{4-}$ and I$^-$, although since this measurement was made in an unbuffered solution without control of the ionic strength, we cannot directly compare the numerical value with that obtained from the kinetic data. The association is slightly exothermic with a positive entropy. This latter effect is likely dominated by the decreased hydration of the product $Pt_2(\mu\text{-}P_2O_5H_2)_4I^{5-}$ as compared to that of the simple iodide ion.

The replacement of chloride ion in $Pt_2(\mu\text{-}P_2O_5H_2)_4Cl_2^{4-}$ by bromide ion shows a similar pathway, except that now the plot of k_{obsd} against $[Pt_2(\mu\text{-}P_2O_5H_2)_4^{4-}]$ is nonlinear and approaches a value independent of $[Pt_2(\mu\text{-}P_2O_5H_2)_4^{4-}]$ at higher concentrations (Figure 3). When k_{obsd} is plotted against [Br$^-$], the plot is linear up to the maximum concentration used. We can interpret this difference from the reaction with iodide ion if the primary mechanistic sequence involves a reaction between $Pt_2(\mu\text{-}P_2O_5H_2)_4^{4-}$ and $Pt_2(\mu\text{-}P_2O_5H_2)_4X_2^{4-}$. Combining these equations leads to the rate law

$$\text{rate} = k_{obsd}[Pt_2(\mu\text{-}P_2O_5H_2)_4Cl_2^{4-}]$$

where

$$k_{obsd} = \frac{k_4K_3[Pt_2(\mu\text{-}P_2O_5H_2)_4^{4-}][Br^-]}{1 + K_3[Pt_2(\mu\text{-}P_2O_5H_2)_4^{4-}]}$$

where the k_c/k_d, k_e/k_f, and k_g/k_h steps are combined to give a single k_4 step. The observed nonlinearity of plots of k_{obsd} against $[Pt_2(\mu\text{-}P_2O_5H_2)_4^{4-}]$ is a consequence of $[Pt_2(\mu\text{-}P_2O_5H_2)_4^{4-}]$ being both in the numerator and denominator of the rate expression. Data analysis gives $K_3 = 1.25 \times 10^5$ M^{-1} and $k_4 = 5.8 \times 10^{-1}$ M^{-1} s^{-1}.

Our results show that replacement of Cl$^-$ in $Pt_2(\mu\text{-}P_2O_5H_2)_4Cl_2^{4-}$ by *both* I$^-$ and Br$^-$ is catalyzed by $Pt_2(\mu\text{-}P_2O_5H_2)_4^{4-}$, but from the curvatures in the k_{obsd} plots, we conclude that $Pt_2(\mu\text{-}P_2O_5H_2)_4^{4-}$ is primarily associated with I$^-$ for the former reaction and with $Pt_2(\mu\text{-}P_2O_5H_2)_4Cl_2^{4-}$ for the latter reaction.

Iodide ion reacts with $Pt_2(\mu\text{-}P_2O_5H_2)_4Br_2^{4-}$ to give $Pt_2(\mu\text{-}P_2O_5H_2)_4I_2^{4-}$ (eq 13). An overlap of the time-lapsed absorption

$$Pt_2(\mu\text{-}P_2O_5H_2)_4Br_2^{4-} + 2I^- \rightarrow Pt_2(\mu\text{-}P_2O_5H_2)_4I_2^{4-} + 2Br^- \quad (13)$$

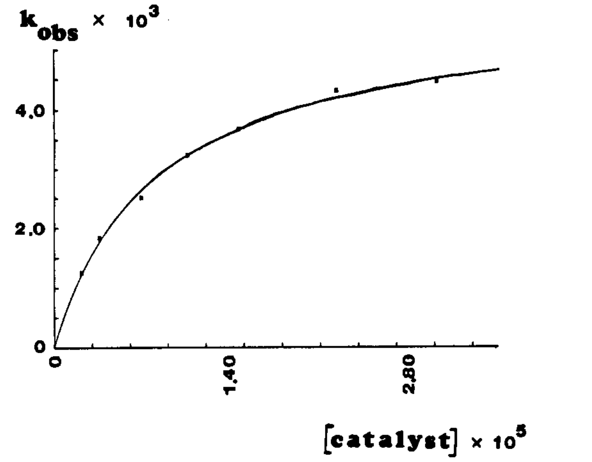

Figure 3. Plot of k_{obsd} against $[Pt_2(\mu\text{-}P_2O_5H_2)_4^{4-}]$ for the reaction of $Pt_2(\mu\text{-}P_2O_5H_2)_4Cl_2^{4-}$ with Br$^-$.

Table IV. k_{obsd} vs $[Pt_2(\mu\text{-}P_2O_5H_2)_4^{4-}]$ for the Reaction of $Pt_2(\mu\text{-}P_2O_5H_2)_4Br_2^{4-}$ with I$^-$ [a]

k_{obsd}, s^{-1}	$[Pt_2(\mu\text{-}P_2O_5H_2)_4^{4-}]$, M
1.83 (±0.04) × 10^{-5}	0
2.75 (±0.05) × 10^{-3}	1.68 × 10^{-6}
8.30 (±0.60) × 10^{-3}	4.19 × 10^{-6}
1.17 (±0.07) × 10^{-2}	6.28 × 10^{-6}
1.18 (±0.05) × 10^{-2}	8.36 × 10^{-6}
1.49 (±0.14) × 10^{-2}	1.04 × 10^{-5}
1.78 (±0.08) × 10^{-2}	1.25 × 10^{-5}
2.18 (±0.04) × 10^{-2}	1.46 × 10^{-5}
2.16 (±0.10) × 10^{-2}	1.66 × 10^{-5}
4.37 (±0.025) × 10^{-2}	3.29 × 10^{-5}

[a] $[Pt_2(\mu\text{-}P_2O_5H_2)_4Br_2^{4-}]_0$ and [I$^-$] are 1.9 × 10^{-5} and 8.0 × 10^{-3} M, respectively; μ = 1.00 M at pH 6.0.

Table V. k_{obsd} vs [I$^-$] for the Reaction of $Pt_2(\mu\text{-}P_2O_5H_2)_4Br_2^{4-}$ with I$^-$ [a]

k_{obsd}, s^{-1}	[I$^-$], M	k_{obsd}, s^{-1}	[I$^-$], M
3.32 (±0.06) × 10^{-3}	3.71 × 10^{-3}	1.00 (±0.05) × 10^{-2}	3.96 × 10^{-2}
3.66 (±0.14) × 10^{-3}	7.43 × 10^{-3}	1.03 (±0.17) × 10^{-2}	4.95 × 10^{-2}
4.30 (±0.18) × 10^{-3}	9.90 × 10^{-3}	1.76 (±0.04) × 10^{-2}	7.43 × 10^{-2}
7.81 (±0.10) × 10^{-2}	1.98 × 10^{-2}	2.31 (±0.03) × 10^{-2}	9.90 × 10^{-2}
8.35 (±0.08) × 10^{-2}	2.97 × 10^{-2}		

[a] $[Pt_2(\mu\text{-}P_2O_5H_2)_4Br_2^{4-}]_0$ and $[Pt_2(\mu\text{-}P_2O_5H_2)_4^{4-}]_0$ are 2.5 × 10^{-5} and 2.66 × 10^{-6} M, respectively; μ = 1.00 M at pH 6.0.

(18) El-Mehdawi, R.; Bryan, S. A.; Roundhill, D. M. *J. Am. Chem. Soc.* **1985**, *107*, 6282–6286.
(19) Hammes, G. G. *Enzyme Catalysis and Regulation*; Academic: New York, 1982; p 165.

Table VI. k_{obsd} vs $[I_2]$ for the Reaction of $Pt_2(\mu\text{-}P_2O_5H_2)_4Cl_2^{4-}$ with I^- [a]

k_{obsd}, s^{-1}	$[I_2]$, M	$[Pt_2(\mu\text{-}P_2O_5H_2)_4Cl_2^{4-}]_0$, M
1.34 (±0.07) × 10^{-4}	0	4.21 × 10^{-5}
6.60 (±1.60) × 10^{-5}	3.64 × 10^{-7}	3.19 × 10^{-5}
2.20 (±0.40) × 10^{-5}	7.30 × 10^{-7}	6.30 × 10^{-5}
1.70 (±0.25) × 10^{-5}	1.81 × 10^{-6}	1.13 × 10^{-5}
8.76 (±0.15) × 10^{-6}	2.70 × 10^{-6}	2.18 × 10^{-5}
8.91 (±0.30) × 10^{-6}	3.58 × 10^{-6}	1.64 × 10^{-5}

[a] $[I^-] = 6.25 \times 10^{-4}$ M; $\mu = 0.110$ M at pH 6.0.

Table VII. k_{obsd} vs $[I^-]$ with High I_2 Concentration for the Reaction of $Pt_2(\mu\text{-}P_2O_5H_2)_4Cl_2^{4-}$ with I^- [a]

k_{obsd}, s^{-1}	$[I^-]$, M	$[Pt_2(\mu\text{-}P_2O_5H_2)_4Cl_2^{4-}]_0$, M
8.91 (±0.3) × 10^{-6}	6.25 × 10^{-4}	1.64 × 10^{-5}
1.47 (±0.4) × 10^{-5}	3.44 × 10^{-3}	1.76 × 10^{-5}
1.76 (±0.4) × 10^{-5}	6.14 × 10^{-3}	1.94 × 10^{-5}
2.88 (±0.7) × 10^{-5}	1.43 × 10^{-2}	1.98 × 10^{-5}

[a] $[I_2] = 3.58 \times 10^{-6}$ M; $\mu = 0.110$ M at pH 6.0.

spectra shows isosbestic points as reactant (λ_{max} = 305 nm) converts to product (λ_{max} = 338 nm), indicative of a transformation with no observable intermediates. When k_{obsd} is plotted against either $[Pt_2(\mu\text{-}P_2O_5H_2)_4^{4-}]$ or $[I^-]$ the correlation is linear up to the maximum concentrations used (Tables IV and V). With no *direct* evidence for inhibition effects at high concentration, we can combine the K_1, K_3, and k_g/k_h steps to give eq 14, followed by a fast conversion of $Pt_2(\mu\text{-}P_2O_5H_2)_4BrI^{4-}$ to the product $Pt_2(\mu\text{-}P_2O_5H_2)_4I_2^{4-}$ (eq 15). Data analysis gives $k = 1.2\ (4) \times 10^5$ $M^{-1}\ s^{-1}$.

$$Pt_2(\mu\text{-}P_2O_5H_2)_4Br_2^{4-} + Pt_2(\mu\text{-}P_2O_5H_2)_4^{4-} + I^- \xrightarrow{k} Pt_2(\mu\text{-}P_2O_5H_2)_4BrI^{4-} + Pt_2(\mu\text{-}P_2O_5H_2)_4^{4-} + Br^- \quad (14)$$

$$Pt_2(\mu\text{-}P_2O_5H_2)_4BrI^{4-} + I^- \xrightarrow{\text{fast}} Pt_2(\mu\text{-}P_2O_5H_2)_4I_2^{4-} + Br^- \quad (15)$$

(b) Uncatalyzed Pathways. In order to probe any slower pathways that are not catalyzed by $Pt_2(\mu\text{-}P_2O_5H_2)_4^{4-}$, we must first remove traces of this complex from the reaction mixtures. We have accomplished this by adding iodine to the reaction solution. The binuclear platinum(II) complex rapidly adds iodine to give $Pt_2(\mu\text{-}P_2O_5H_2)_4I_2^{4-}$, and since iodine does not react with $Pt_2(\mu\text{-}P_2O_5H_2)_4Cl_2^{4-}$,[13] we have available a selective method for the removal of $Pt_2(\mu\text{-}P_2O_5H_2)_4^{4-}$. Since the amount of added I_2 is small compared to $[I^-]$, the species I_3^- is not present in sufficient concentration to compete with I^- as the entering group. Using this method, we have studied the kinetics of the reaction of $Pt_2(\mu\text{-}P_2O_5H_2)_4Cl_2^{4-}$ with iodide ion. In Table VI we show our k_{obsd} data with added I_2. These data verify that there is a rapid initial drop in the value of k_{obsd}, which then levels to a saturation limit when $Pt_2(\mu\text{-}P_2O_5H_2)_4^{4-}$ has been effectively removed from the solution. Working at this saturation level with respect to iodine-induced catalyst suppression, we have measured k_{obsd} for different values of $[I^-]$. These data are given in Table VII. We have obtained the values of $k_{associative}$ from the slope, and $k_{dissociative}$ from the intercept of these graphed data. These respective values are 1.4 (2) × 10^{-3} $M^{-1}\ s^{-1}$ and 8.9 (10) × 10^{-6} s^{-1}. Dissociative chloride ion loss from $Pt_2(\mu\text{-}P_2O_5H_2)_4Cl_2^{4-}$ therefore makes only a minimal kinetic concentration to the overall rate of substitution of chloride by iodide ion.

Two mechanisms can be used to account for the bimolecular associative pathway. The simplest pathway would involve direct attack by iodide ion at a platinum(III) center in $Pt_2(\mu\text{-}P_2O_5H_2)_4Cl_2^{4-}$. This mechanism is required to involve frontside attack at the diplatinum(III) complex $Pt_2(\mu\text{-}P_2O_5H_2)_4Cl_2^{4-}$, followed by associative interchange between iodide and chloride ions at the *pseudo* 7-coordinate intermediate. Such a mechanism has long been considered unlikely for monomeric complexes of platinum(IV), and an associative attack by the incoming halide ion at the coordinated halogen ligand in the complex is the favored mechanism. Our second-order pathway in the controlled absence of $Pt_2(\mu\text{-}P_2O_5H_2)_4^{4-}$ also correlates with such a reductive-elimination–oxidative-addition (REOA) mechanism. In this mechanism the iodide nucleophile directly attacks at the coordinated axial chloride ligand, thereby inducing reductive elimination (eq 16).[20] Subsequent oxidative addition of ICl followed by a second

$$I^-\ Cl\text{–}Pt\text{–}Pt\text{–}Cl^{4-} \rightarrow I\text{–}Cl + Pt\ Pt^{4-} + Cl^- \quad (16)$$

REOA pathway on the chloride ligand of $Pt_2(\mu\text{-}P_2O_5H_2)_4ICl^4$ gives the product $Pt_2(\mu\text{-}P_2O_5H_2)_4I_2^{4-}$ (eq 17 and 18).

$$Pt\ Pt^{4-} + ICl \rightarrow I\text{–}Pt\text{–}Pt\text{–}Cl^{4-} \quad (17)$$

$$I^- + Cl\text{–}Pt\text{–}Pt\text{–}I \rightarrow I\text{–}Pt\text{–}Pt\text{–}I + Cl^- \quad (18)$$

We cannot unambiguously distinguish between the associative interchange and REOA pathways. No direct evidence has been found for the formation if ICl in the reaction, nor do we expect any attempts to detect it to be successful. Either reaction 17 will be very fast, or ICl will rapidly react with iodide ion to give I_2, which is already present in the reaction mixture.

The slowest pathway follows a rate law independent of $[I^-]$. This pathway correlates with a dissociative mechanism involving slow chloride ion replacement by water, followed by rapid substitution of the axial water ligand by iodide ion. Repeating the sequence with the intermediate $Pt_2(\mu\text{-}P_2O_5H_2)_4ClI^{4-}$ gives the final product $Pt_2(\mu\text{-}P_2O_5H_2)_4I_2^{4-}$ (eq 19 and 20). Since the value for

$$Pt_2(\mu\text{-}P_2O_5H_2)_4Cl_2^{4-} \xrightarrow[-Cl^-]{H_2O} Pt_2(\mu\text{-}P_2O_5H_2)_4Cl(H_2O)^{3-} \xrightarrow[-H_2O]{I^-} Pt_2(\mu\text{-}P_2O_5H_2)_4ClI^{4-} \quad (19)$$

$$Pt_2(\mu\text{-}P_2O_5H_2)_4ClI^{4-} \xrightarrow[-Cl^-]{H_2O} Pt_2(\mu\text{-}P_2O_5H_2)_4I(H_2O)^{3-} \xrightarrow[H_2O]{I^-} Pt_2(\mu\text{-}P_2O_5H_2)_4I_2^{4-} \quad (20)$$

$k_{dissociative}$ is obtained by following the loss of $Pt_2(\mu\text{-}P_2O_5H_2)_4Cl_2^{4-}$, the measured constant is that for the first step in eq 19.

Comparison with Monomeric Platinum(II) and Platinum(IV) Complexes. The mechanistic pathways for the substitution of X^- by Y^- in $Pt_2(\mu\text{-}P_2O_5H_2)_4X_2^{4-}$ show all the qualitative features previously found in monomeric kinetically inert octahedral platinum(IV) complexes. These features are the observation of platinum(II) catalysis, the presence of a bimolecular associative or REOA pathway, and the occurrence of a very slow dissociative mechanism.

Quantitatively the μ-pyrophosphito diplatinum(III) complexes show differences from monomeric platinum(IV) complexes. We observe a leaving group order $Cl^- > Br^- \gg I^-$ in the complexes $Pt_2(\mu\text{-}P_2O_5H_2)_4X_2^{4-}$. The inertness of $Pt_2(\mu\text{-}P_2O_5H_2)_4I_2^{4-}$ is clearly evidenced by the observation that we detect no substitution of I^- by Cl^- in $Pt_2(\mu\text{-}P_2O_5H_2)_4I_2^{4-}$ even after several days at 25 °C in a solution of pH 6. The entering group order follows the sequence $I^- > Br^- > Cl^-$. For *monomeric* platinum(IV) complexes, however, both the leaving and entering group orders are $Br^- > Cl^- > I^-$.[15,16,21] It is apparent that these diplatinum(III) complexes show qualitative kinetic behavior analogous to that of platinum(IV) complexes but our observed leaving group order of $Cl^- > Br^- > I^-$ does not follow that found for monomeric platinum(II)-catalyzed substitutions in platinum(IV) complexes. The order in reversal between Cl^- and Br^- indicates that the chloride ion may more

(20) Chanon, M.; Tobe, M. L. *Angew. Chem., Int. Ed. Engl.* **1982**, *21*, 1–23. Zvyagintsev, O. E.; Shubochkina, E. F. *Russ. J. Inorg. Chem.* (*Engl. Transl.*) **1961**, *6*, 1038–1042. Zvyagintsev, O. E.; Shubochkina, E. F. *Russ. J. Inorg. Chem.* (*Engl. Transl.*) **1963**, *8*, 300–304. Poë, A. J.; Vaidya, M. S. *J. Chem. Soc.* **1960**, 187–191. Poë, A. J.; Vaidya, M. S. *Proc. Chem. Soc., London* **1960**, 118–119. Poë, A. J.; Vaidya, M. S. *J. Chem. Soc.* **1961**, 2981–2987. Johnson, R. C.; Berger, E. R. *Inorg. Chem.* **1965**, *4*, 1262–1264. Johnson, R. C.; Berger, E. R. *Inorg. Chem.* **1968**, *7*, 1656–1659. Bounsall, E. J.; Hewkin, D. J.; Hopgood, D.; Poë, A. J. *Inorg. Chim. Acta* **1967**, *1*, 281–286. Johnson, D. W.; Poë, A. J. *Can. J. Chem.* **1974**, *52*, 3083–3086.
(21) Basolo, F.; Pearson, R. G. *Mechanisms of Inorganic Reactions*, 2nd ed.; Wiley: New York, 1967.

Table VIII. Thermal and Photochemical Halide Substitution Reaction of $Pt_2(\mu\text{-}P_2O_5H_2)_4X_2^{4-}$ with Halides Y^-

complex	halide	conditions	time	% substn
$Pt_2(\mu\text{-}P_2O_5H_2)_4Cl_2^{4-}$	I^-	thermal	200 m	75
		$h\nu$	70 s	75
	Br^-	thermal	3 h	0
		$h\nu$	60 s	60
$Pt_2(\mu\text{-}P_2O_5H_2)_4Br_2^{4-}$	I^-	thermal	12 h	1
		$h\nu$	12 m	75
	Cl^-	thermal	12 h	4
		$h\nu$	12 m	60
$Pt_2(\mu\text{-}P_2O_5H_2)_4I_2^{4-}$	Br^-	thermal	3 h	3
		$h\nu$	2 m	95
	Cl^-	thermal	3 days	0
		$h\nu$	15 m	100

Table IX. Quantum Yields for the Photoreactions of $Pt_2(\mu\text{-}P_2O_5H_2)_4Cl_2^{4-}$ with I^- To Give $Pt_2(\mu\text{-}P_2O_5H_2)_4I_2^{4-}$ [a]

conditions			quantum yields
pH	$[I^-]$, M	other	Φ_{Cl_2} [b]
0.94[c]	1×10^{-4}	1×10^{-1} M Cl^-	$2.5\ (\pm0.6) \times 10^{-4}$
1.50[d]	1×10^{-1}		$1.8\ (\pm0.5) \times 10^{-3}$
1.50[d]	1×10^{-1}	$\sim10^{-4}$ M I_2	$2.8\ (\pm0.8) \times 10^{-3}$

[a] $[Pt_2(\mu\text{-}P_2O_5H_2)_4Cl_2]_0$ are 1×10^{-5} to 5×10^{-5} M. All reactions were irradiated at 286 nm. [b] Φ_{Cl_2} = quantum yield based on the loss of reactant $Pt_2(\mu\text{-}P_2O_5H_2)_4Cl_2^{4-}$; concentrations were measured spectrophotometrically. [c] pH of HCl reaction mixture prior to addition of reactants. [d] pH of phosphoric acid reaction mixture prior to addition of reactants.

Table X. Quantum Yields for the Photoreaction of $Pt_2(\mu\text{-}P_2O_5H_2)_4I_2^{4-}$ with Cl^- To Give $Pt_2(\mu\text{-}P_2O_5H_2)_4ClI^{4-}$ [a]

conditions			quantum yields
pH	$[Cl^-]$, M	other	Φ_{I_2} [b]
0.94[c]	0.11		$5.2\ (\pm1) \times 10^{-4}$
1.00[c]	0.10		$2.2\ (\pm0.2) \times 10^{-4}$
1.00[c]	0.10	*e*	$1.5\ (\pm0.2) \times 10^{-4}$
6.00[d]	0.10		$2.3\ (\pm0.6) \times 10^{-5}$

[a] $[Pt_2(\mu\text{-}P_2O_5H_2)_4I_2^{4-}]$ are 5×10^{-6} to 2.5×10^{-5} M. Reactions were irradiated at 338 nm. [b] Φ_{I_2} = quantum yield based on the loss of reactant $Pt_2(\mu\text{-}P_2O_5H_2)_4I_2^{4-}$. Product concentrations were determined spectrophotometrically. [c] pH of the HCl reaction solution before addition of the complex. [d] Phosphate buffer solution, μ = 0.11 M. [e] 3×10^{-4} M Fe^{3+} added as $K_3Fe(CN)_6$.

effectively form a bridge in these μ-pyrophosphito diplatinum complexes than it does with the monomeric systems.

Photoinduced Substitution Reactions. The rate of substitution of X^- by Y^- in the complexes $Pt_2(\mu\text{-}P_2O_5H_2)_4X_2^{4-}$ is markedly accelerated by light; hence, these thermal kinetic data have been collected with all light excluded. When reaction mixtures containing $Pt_2(\mu\text{-}P_2O_5H_2)_4X_2^{4-}$ and Y^- are photolyzed with a 200-W mercury lamp ($\lambda_{max} > 335$ nm) we observe over a hundredfold increase in the rate of formation of substitution product. The comparison between thermal and photochemical yields of products are collected in Table VIII. We have measured the quantum yields for the reactions shown in eq 21 and have collected these

$$Pt_2(\mu\text{-}P_2O_5H_2)_4Cl_2^{4-} \underset{h\nu,\ Cl^-}{\overset{h\nu,\ I^-}{\rightleftharpoons}} Pt_2(\mu\text{-}P_2O_5H_2)_4ClI^{4-} \underset{h\nu,\ Cl^-}{\overset{h\nu,\ I^-}{\rightleftharpoons}} Pt_2(\mu\text{-}P_2O_5H_2)_4I_2^{4-} \quad (21)$$

data in Tables IX and X. All the quantum yields are small, falling in the range of 10^{-3}–10^{-6}. Under strongly acidic conditions (pH $\approx$1), where the rate of thermal halide replacement is negligibly slow, we can observe the sequential formation of first the mixed-halide complex and then the symmetrically substituted dihalo product. In particular we have studied the photoinduced conversion of $Pt_2(\mu\text{-}P_2O_5H_2)_4I_2^{4-}$ into $Pt_2(\mu\text{-}P_2O_5H_2)_4ClI^{4-}$ and then $Pt_2(\mu\text{-}P_2O_5H_2)_4Cl_2^{4-}$ with added HCl (pH 1) and the reverse replacement of chloride by iodide ion (eq 21). Clearly the observed

Table XI. Quantum Yields for the Photoassisted Reductive Elimination of X_2 from $Pt_2(\mu\text{-}P_2O_5H_2)_4X_2^{4-}$ (X = Cl, Br, I)[a]

reactant complex	wavelength irradiated, nm	Φ_{Pt_2}
$Pt_2(\mu\text{-}P_2O_5H_2)_4Cl_2^{4-}$	286	$7.3\ (\pm1) \times 10^{-4}$
$Pt_2(\mu\text{-}P_2O_5H_2)_4Br_2^{4-}$	310	$1.8\ (\pm1) \times 10^{-4}$
$Pt_2(\mu\text{-}P_2O_5H_2)_4I_2^{4-}$	338	$1.1\ (\pm1) \times 10^{-5}$

[a] pH 6.0, μ = 0.11 M. No free halide added. Reactant complex concentrations range from 4×10^{-5} to 5×10^{-5} M. Φ_{Pt_2} is the quantum yield based on the formation of $Pt_2(\mu\text{-}P_2O_5H_2)_4^{4-}$.

photoenhancement of the substitution reactions is not a consequence of high quantum yields but is caused by the large extinction coefficients ($\sim 4 \times 10^4$ M^{-1} cm^{-1}) of the irradiated chromophores; consequently, the amount of light being absorbed will be large, and therefore the extent of overall photoconversion can be high.

Mechanistically three pathways are plausible. The first pathway involves an initial photoinduced reductive elimination of halogen from $Pt_2(\mu\text{-}P_2O_5H_2)_4X_2^{4-}$, when the formed complex $Pt_2(\mu\text{-}P_2O_5H_2)_4^{4-}$ is a thermal catalyst for halide-substitution reactions. This pathway can be eliminated for the conversion of $Pt_2(\mu\text{-}P_2O_5H_2)_4I_2^{4-}$ into $Pt_2(\mu\text{-}P_2O_5H_2)_4Cl_2^{4-}$ in HCl (pH 1) because no such thermal reaction is observed in the presence of excess $Pt_2(\mu\text{-}P_2O_5H_2)_4^{4-}$. In this context we find that the quantum yields for the photoinduced reductive elimination of halogen X_2 from $Pt_2(\mu\text{-}P_2O_5H_2)_4X_2^{4-}$ are small (Table XI). Two other pathways are realistic. These involve either initial halogen atom loss from $Pt_2(\mu\text{-}P_2O_5H_2)_4X_2^{4-}$ to give $Pt_2(\mu\text{-}P_2O_5H_2)_4X^{4-}$ or the photomolysis of the diplatinum(III) bond. The first pathway corresponds to the Taube mechanism for photosubstitution of $PtCl_6^{2-}$ with bromide ion.[22] In the Taube mechanism with monomeric Pt(IV) complexes the quantum yields are high (100–2000), and the addition of $Fe(CN)_6^{3-}$ inhibits the photoreaction. For the $Pt_2(\mu\text{-}P_2O_5H_2)_4X_2^{4-}$ complexes the quantum yields are low (Tables IX and X), and there is no inhibition with $Fe(CN)_6^{3-}$. Our photolysis data are best explained if the initial photoprocess is Pt(III)–Pt(III) bond homolysis by absorption of light into the $d_\sigma \rightarrow d_{\sigma^*}$ chromophore. Bond homolysis will create a $d_\sigma{}^1d_{\sigma^*}{}^1$ excited state where each platinum(III) center is formally a 17-electron ion. Furthermore it is to be expected that promotion of an electron into $d_{z^2}{}^*$ orbital will lead to *selective* labilization of axial halide substituents. This premise is based on the prediction of the simplified molecular orbital model that this d_{σ^*} electron will be located along the intermetallic *z* axis. Quantum yields for such a mechanism would be expected to be very low because rapid recombination to form the intermetallic σ bond is to be expected. Recently, however, it has been shown that the $d_\sigma{}^1d_\sigma{}^{*1}$ triplet excited state of $Pt_2(\mu\text{-}P_2O_5H_2)_4X_2^{4-}$ has a sufficiently long lifetime ($\sim$20 μs) for photolabilization to occur from this excited state, even if the mechanism involves an associative hydration pathway with the solvent.[23] Apparently the photochemically formed diradical from $Pt_2(\mu\text{-}P_2O_5H_2)_4X_2^{4-}$ has a long lifetime because relaxation back to the ground state requires a triplet–singlet spin change and the formation of a Pt–Pt bond. The subsequent contraction of the Pt–Pt separation of 0.2 Å will involve considerable reorganizational changes in the torsion energies within the bridging ligands. These differences in nonbonded interactions will contribute to the long lifetime of the diradical ($d\sigma^1d\sigma^{*1}$) excited state.

Conclusions. 1. The diplatinum(III) complexes $Pt_2(\mu\text{-}P_2O_5H_2)_4X_2^{4-}$ undergo substitution of X^- by added halide ion Y^-

(22) Rich, R. L.; Taube, H. *J. Am. Chem. Soc.* **1954**, *76*, 2608–2611. Taube, H. *Chem. Rev.* **1952**, *50*, 69–126. Herschel, J. F. W. *Philos. Mag. J. Sci.* **1832**, *1*, 58–60. Archibald, E. H. *J. Chem. Soc., Trans.* **1920**, *117*, 1104–1120. Adamson, A. W.; Sporer, A. H. *J. Am. Chem. Soc.* **1958**, *80*, 3865–3870. Julliard, M.; Chanon, M. *Chem. Rev.* **1983**, *83*, 425–506. Wright, R. C.; Lawrence, G. S. *J. Chem. Soc., Chem. Commun.* **1972**, 132–133. Adams, G. E.; Broszkiewicz, R. B.; Michael, B. D. *Trans. Faraday Soc.* **1968**, *64*, 1256–1264. Dreyer, R.; Koenig, K.; Schmidt, H. *Z. Phys. Chem. (Leipzig)* **1964**, *17*, 257–271. Dreyer, R. *Z. Phys. Chem. (Frankfurt)* **1961**, *29*, 347–355. Dreyer, R. *Kernenergie* **1962**, *5*, 618–621. Dreyer, R.; Koenig, K. *Z. Chem.* **1966**, *6*, 271.
(23) Stiegman, A. E.; Miskowski, V. M.; Gray, H. B. *J. Am. Chem. Soc.* **1986**, *108*, 2781–2782.

by a combination of mechanisms including a $Pt_2(\mu\text{-}P_2O_5H_2)_4^{4-}$-catalyzed pathway, a slower bimolecular substitution mechanism, and a very slow dissociative pathway. By contrast the μ-hydrogen phosphato complexes $Pt_2(\mu\text{-}PO_4H)_4X_2^{4-}$ have labile axial halides that undergo rapid hydration.

2. The kinetic data indicate association between $Pt_2(\mu\text{-}P_2O_5H_2)_4^{4-}$ and either I^- or $Pt_2(\mu\text{-}P_2O_5H_2)_4Cl_2^{4-}$.

3. The replacement of X^- in $Pt_2(\mu\text{-}P_2O_5H_2)_4X_2^{4-}$ by Y^- is photoaccelerated. Dissociation from the triplet $d\sigma^1 d\sigma^{*1}$ state is selectively axial.

4. The substitution reactions of $Pt_2(\mu\text{-}P_2O_5H_2)_4X_2^{4-}$ show qualitative similarity to those of monomeric platinum(IV) complexes, there being no abnormal kinetic effects induced by the diplatinum(III) bonds.

Acknowledgment. We thank A. J. Poë for his critical reading of our manuscript and R. H. Schmehl for helpful discussions. We thank the donors of the Petroleum Research Fund, administered by the American Chemical Society, for partial support of this research.

Supplementary Material Available: Appendices detailing the rate law derivations, a spectral overlay, and several plots of k_{obsd} against complex or halide ion concentrations (10 pages). Ordering information is given on any current masthead page.

Contribution from the Department of Chemistry, University of Oregon, Eugene, Oregon 97403, and Central Research and Development Department, Experimental Station, E. I. du Pont de Nemours and Company, Wilmington, Delaware 19898

Trivacant Heteropolytungstate Derivatives. 3.[1] Rational Syntheses, Characterization, Two-Dimensional ^{183}W NMR, and Properties of $P_2W_{18}M_4(H_2O)_2O_{68}^{10-}$ and $P_4W_{30}M_4(H_2O)_2O_{112}^{16-}$ (M = Co, Cu, Zn)

Richard G. Finke,*[2a] Michael W. Droege,[2a] and Peter J. Domaille[2b]

Received May 21, 1987

The full details are reported on the rational, high-yield, and isomerically pure syntheses of $P_2W_{18}M_4(H_2O)_2O_{68}^{10-}$ and $P_4W_{30}M_4(H_2O)_2O_{112}^{16-}$ ($M = Co^{2+}, Cu^{2+}, Zn^{2+}$). The products are well-characterized, including 2-D ^{183}W NMR in the case of $M = Zn^{2+}$, which allows the unambiguous assignment of the ^{183}W NMR spectra. The results allow a number of conclusions to be drawn: (i) the B-type tri(tungsten)vacant form of B-$PW_9O_{34}^{9-}$ and B-$P_2W_{15}O_{56}^{12-}$ is a key structural requirement for formation of the dimetal(2+)-substituted dimers $P_2W_{18}M_4(H_2O)_2O_{68}^{10-}$ and $P_4W_{30}M_4(H_2O)_2O_{112}^{16-}$; (ii) these disubstituted dimers are not unique but rather are just the first two members of a conceptually more general, previously unrecognized class of heteropolyanions; (iii) the Cu^{2+} product $P_2W_{18}Cu_4(H_2O)_2O_{68}^{10-}$ is different from the M^{2+} = Zn, Co members as well as different from $P_4W_{30}Cu_4(H_2O)_2O_{112}^{16-}$ in that it is thermally unstable in solution; (iv) both $PW_9O_{34}^{9-}$ and $P_4W_{30}Zn_4(H_2O)_2O_{112}^{16-}$ undergo previously unknown solid-state isomerizations; (v) the complex previously reported as "$P_2W_{16}M_2(H_2O)_2O_{60}^{10-}$" was misformulated and is in fact $P_4W_{30}M_4(H_2O)_2O_{112}^{16-}$. Additional results and conclusions are detailed in the text and in the Summary and Conclusions.

Introduction

In 1973 Weakley, Evans, Showell, Tourné, and Tourné isolated[3] $K_{10}P_2W_{18}Co_4(H_2O)_2O_{68}$ from the prolonged reaction of a 11:2:4:18 mixture of $HCl/Na_2HPO_4/Co(NO_3)_2/Na_2WO_4$ at 90–100 °C and determined its structure by X-ray diffraction (Figure 1A). Beginning in 1979, as part of our initial efforts[1a,b] aimed at preparing the series of trimetal (M)-substituted heteropolyanions $SiW_9M_3O_{40}^{x-}$ and $P_2W_{15}M_3O_{62}^{y-}$ (Figure 2) for use as organic-solvent-soluble metal oxide analogues in catalysis,[1c] we attempted the synthesis of "$PW_9(ZnO)_3O_{34}^{9-}$", a potential ZnO analogue.[4] Despite the fact that the trisubstituted Co^{2+} derivative $(Me_4N)_{10}SiW_9Co_3(H_2O)_3O_{34}\cdot 10H_2O$ apparently exists,[4d,5] a spectral titration using Co^{2+} in place of Zn^{2+} with $PW_9O_{34}^{9-}$ in

(1) (a) Part 1: Finke, R. G.; Droege, M.; Hutchinson, J. R.; Gansow, O. *J. Am. Chem. Soc.* **1981**, *103*, 1587–1589. (b) Part 2: Finke, R. G.; Droege, M. W. *Inorg. Chem.* **1983**, *22*, 1006–1008. (c) For part 1 of our work on "Trisubstituted Heteropolyanions as Soluble Metal Oxide Analogues", see: Finke, R. G.; Droege, M. W. *J. Am. Chem. Soc.* **1984**, *106*, 7274–7277. For part 2 see: Finke, R. G.; Rapko, B. M.; Domaille, P. J. *Organometallics* **1986**, *5*, 175. For part 3 see: Finke, R. G.; Rapko, B. M.; Saxton, R. J.; Domaille, P. J. *J. Am. Chem. Soc.* **1986**, *108*, 2947. For part 4 see: Edlund, D. J.; Finke, R. G., submitted for publication in *Organometallics*.

(2) (a) University of Oregon. (b) E. I. du Pont de Nemours and Company; Contribution No. 3965.

(3) (a) Weakley, T. J. R.; Evans, H. T., Jr.; Showell, J. S.; Tourné, G. F.; Tourné, C. M. *J. Chem. Soc., Chem. Commun.* **1973**, 139–140. Although a yield was not reported, repeating their synthesis provided 3.1 g (29%) of this product along with 1.3 g of a blue insoluble byproduct.[1a] A deep rose-pink crystalline byproduct from this synthesis has been identified by a single-crystal X-ray diffraction analysis[26] as $P_5Co_9W_{27}O_{119}H_{17}^{16-}$. (b) Professor Weakley has kindly provided us with a preprint of a follow-up full paper concerning this work: Evans, H. T., Jr.; Tourné, C. M.; Tourné, G. F.; Weakley, T. J. R. *J. Chem. Soc., Dalton Trans.* **1986**, 2699. Described therein are the full details of their syntheses and of the original[3a] $P_2W_{18}Cu_4(OH_2)_2O_{68}^{10-}$ and now $As_2W_{18}Zn_4(OH_2)_2O_{68}^{10-}$ X-ray diffraction structural analyses and the ^{183}W NMR spectrum of $P_2W_{18}Zn_4(OH_2)_2O_{68}^{10-}$ (see also Table I *herein*).

(4) (a) We chose to try to mimic ZnO initially because ZnO is one of the best characterized examples among oxides as far as surface intermediates and reaction mechanisms are concerned[4b] (in large part due to the good IR properties of ZnO) and because the $(ZnO)_3$ zinc oxide "minisurface" in "$PW_9(ZnO)_3O_{34}^{9-}$" closely resembles the $000\bar{1}$ or polar plane of ZnO.[4c] Our focus on trisubstituted heteropolyanions like $SiW_9M_3O_{40}^{x-}$ is derived in part from the fact that such a trisubstituted heteropolyanion offers the largest possible planar M_xO_y (e.g. Zn_3O_3) minisurface on the Keggin, $XW_{12}O_{40}^{n-}$, anion. Other design features include a high surface charge density, the possibility of A- vs B-type $XW_9M_3O_{40}^{n-}$ comparisons, high (C_{3v}) symmetry simplifying spectroscopic properties, the ^{183}W, X = ^{31}P, ^{29}Si, and M = ^{51}V NMR handles, and the possibility of the comparative series of $SiW_9M_3O_{40}^{x-}$ and $P_2W_{15}M_3O_{40}^{y-}$ for $M = V^{5+}, Nb^{5+}, Ta^{5+}$ and $Ti^{4+}, Zr^{4+}, Hf^{4+}$. For further details see ref 1c. (b) John, C. S. In *Catalysis*; Kemball, G., Dowden, D. A., Eds.; The Chemical Society: London, 1980; Vol. 3, pp 169, 187. (c) Gay, R. R.; Nodine, M. H.; Henrich, V. E.; Zeiger, H. J.; Solomon, E. I. *J. Am. Chem. Soc.* **1980**, *102*, 6752. See Figure 1 therein. (d) The high anionic charge, the large size of Zn^{2+} vs the size of the lacunary hole in $PW_9O_{34}^{9-}$, and the apparent high stability of $P_2W_{18}Zn_4(H_2O)_2O_{68}^{10-}$ are factors that appear to mitigate against the, as yet unknown, $PW_9(ZnO)_3O_{34}^{9-}$ (or $PW_9(ZnOH_2)_3O_{37}^{9-}$), although $SiW_9(CoOH_2)_3O_{37}^{10-}$ has been reported in a preliminary communication.[5]

(5) Katsoulis, D. E.; Pope, M. T. *J. Am. Chem. Soc.* **1984**, *106*, 2737.

0020-1669/87/1326-3886$01.50/0